



## BIOMEDICAL SCIENCES

# TiO<sub>2</sub> Nanocrystals and *Annona crassiflora* Polyphenols Used Alone or Mixed Impact Differently on Wound Repair

FRANCYELLE B.R. DE MOURA, BRUNO ANTONIO FERREIRA, ELUSCA HELENA MUNIZ, RINARA A. SANTOS, JOSÉ AUGUSTO L. GOMIDE, ALLISSON B. JUSTINO, ANIELLE CHRISTINE A. SILVA, NOELIO O. DANTAS, DANIELE L. RIBEIRO, FERNANDA A. ARAÚJO, FOUED S. ESPINDOLA & TATIANA CARLA TOMIOSSO

**Abstract:** Wounds treated with TiO<sub>2</sub> nanoparticles (TiO<sub>2</sub>-NPs) show an improvement in healing time. However, little is known about the parameters that can contribute to this result. On the other hand, the treatment of wounds with polyphenols is widely known. These compounds are found in the peel of *Annona crassiflora* fruit and have antioxidant, analgesic and anti-inflammatory properties. In this study, we evaluated the healing effect of TiO<sub>2</sub> nanocrystals (TiO<sub>2</sub>-NCs), polyphenolic fractions obtained from ethanolic extract of *A. crassiflora* fruit peel (PFAC) and mix (PFAC + TiO<sub>2</sub>-NCs) on the parameters of wound closure, inflammation, collagen deposition, metalloproteinase activity (MMPs) and angiogenesis. TiO<sub>2</sub>-NCs and PFAC have activity for wound healing, showed anti-inflammatory action and a shorter wound closure time. These treatments also contributed to increased collagen deposition, while only treatment with TiO<sub>2</sub>-NCs increased MMP-2 activity, parameters essential for the migration of keratinocytes and for complete restoration of the injured tissue. The combination of PFAC + TiO<sub>2</sub>-NCs reduced the effectiveness of individual treatments by intensifying the inflammatory process, in addition to delaying wound closure. We conclude that the interaction between the hydroxyl groups of PFAC polyphenols with TiO<sub>2</sub>-NCs may have contributed to difference in the healing activity of skin wounds.

**Key words:** TiO<sub>2</sub>, Annonaceae, interactions, Polyphenols, skin wounds.

## INTRODUCTION

Titanium dioxide nanoparticles (TiO<sub>2</sub>-NPs) have been applied in the biomedical area due to their strong oxidation, antibacterial capacity and safety (Fan et al. 2016). The reactive oxygen species (ROS) released in response to the catalytic activity of TiO<sub>2</sub>-NPs is one of the factors related to its antimicrobial (Archana et al. 2013, Osumi et al. 2017) and healing activities (Haugen & Lyngstadaas 2016, Osumi et al. 2017, Sankar et al. 2014). The healing effect of TiO<sub>2</sub>-NPs is often associated with the shorter time required for

wound closure (Sivaranjani & Philominathan 2016).

TiO<sub>2</sub> is a polymorphic material with three allotropic phases, namely anatase, brookite, and rutile (Reyes-Coronado et al. 2008). Considering its safety for application in biological tests, crystalline nanoparticles (nanocrystals) are safer than amorphous nanoparticles (Reis et al. 2016). In addition, the allotropic phases of rutile with brookite nanocrystals are safer than other evaluated associations (Reis et al. 2016). Thus, in this study, we synthesized and characterized

TiO<sub>2</sub>-NCs with mixed of rutile and brookite phases.

Medicinal plants have been used as a therapeutic alternative for many years and still today by about 80% of the population in developing countries (Ekor 2014). Bioactive compounds derived from medicinal plants have been used, in addition to their natural form, also for the development of new chemicals for the pharmaceutical industry (Georgescu et al. 2016). Among the medicinal compounds used in the treatment of wounds are polyphenols found in peel of the fruit of *Annona crassiflora* Mart (De Moura et al. 2019, Justino et al. 2016). In our studies with polyphenols enriched fractions of the fruit peel of *A. crassiflora* (PFAC), we showed its antioxidant potential and in the reduction of non-enzymatic glycation and lipid peroxidation. We also show that PFAC has hepatoprotective activity reducing the effects of Diabetes induced by streptozotocin, in the oxidative stress of liver tissue. PFAC has also been shown to be effective in reducing the inflammatory and nociceptive response in acute and persistent inflammatory pain. In addition, PFAC showed pro-fibrogenic and anti-inflammatory activity in skin repair (De Moura et al. 2019, Justino et al. 2019).

The association of organic molecules such as those found in natural or synthetic products with inorganic nanoparticles can affect both the native properties of organic molecules and influence properties of inorganic subunits, such as in the case of crystalline TiO<sub>2</sub> nanoparticles. This interaction can modify the activities of the components observed individually in relation to the ability to activate, regulate or inhibit biological targets (Khan et al. 2017, Krychowiak et al. 2014, Leu et al. 2012, Prochowicz et al. 2017). Studies showed a significant acceleration of skin wound healing through anti-inflammatory and antioxidant effects when treated by mixing gold nanoparticles with epigallocatechin gallate

flavonoid and  $\alpha$ -lipoic acid (Leu et al. 2012). In addition, a synergistic effect of the interaction between a plant extract with silver nanoparticles enhancing bactericidal activity was also added (Krychowiak et al. 2014). Thus, this study aimed to elucidate the role of TiO<sub>2</sub>-NCs and PFAC, separately, and associated (TiO<sub>2</sub>-NC+PFAC) in the essential processes for wound healing.

## MATERIALS AND METHODS

### Synthesis and characterization of TiO<sub>2</sub> Nanocrystals

TiO<sub>2</sub>-NCs were synthesized based on the methodology (Reis et al. 2016), with a thermal annealing at 800°C/h. High-resolution transmission electron microscopy (HRTEM) images were obtained by high-resolution transmission electron microscopy of accelerating voltage 200 kV, JEOL S100D. The X-ray diffraction (XRD) was recorded with a DRX-6000 (Shimadzu) using monochromatic radiation Cu-K $\alpha$ 1 ( $\lambda=1.54,056 \text{ \AA}$ ) to confirm the formation of TiO<sub>2</sub> NCs, as well as the crystal structure, and average mass fraction of the phase. Micro-Raman spectra were obtained using as excitation source the 780 nm line of an Ocean Optics spectrometer. All characterizations were performed at room temperature.

### Obtaining the fruits peel of *A. crassiflora* ethanolic extracted and the polyphenol-rich fractions

*A. crassiflora* was identified and a sample of the species was deposited in the Herbarium Uberlandense under registration number (HUFU68467). Ethanolic extraction of the peel of these fruits was initially produced (De Moura et al. 2019) and posteriorly soluble in 200 mL of methanol: water (9:1 v-1) and then subjected to a liquid-liquid fractionation (extraction with 200 ml of each solvent) to obtain the fractions

n-butanol and ethyl acetate (Justino et al. 2016). The solvents used in the production of the partitions were removed with a rotary evaporator in a water bath at 40°C and reduced pressure (Rotavapor R-210). The fractions were frozen and lyophilized to remove the remaining water. A mixture of equal parts of the two fractions was used for the *in vivo* assays. Due to the high content of polyphenols presented in both fractions (De Moura et al. 2019, Justino et al. 2016) this mixture was named polyphenols from the fruit of *A. crassiflora* (PFAC).

### Preparing the ointment

The TiO<sub>2</sub>-NCs and PFAC before being added to the vehicle for the preparation of the ointment, were mixed by solvation until obtaining a homogeneous mixture in the form of a fine powder. For the formulation of PFAC + TiO<sub>2</sub>-NCs this procedure was performed with the compositions of the fractions (w / v) of n-butanol (2%) and ethyl acetate (2%) and TiO<sub>2</sub>-NCs (1%). This same proportion was used for the formulation of the individual components (PFAC and TiO<sub>2</sub>-NCs). Then, the ointments of TiO<sub>2</sub>-NCs, PFAC and PFAC + TiO<sub>2</sub> were prepared using the addition of petroleum jelly (30%) and lanolin (70%) until a homogeneous mixture of the ointments was obtained.

### Experiment and distribution of animal groups

Animal testing procedures were approved by the Ethics Commission on Animal Use from Federal University of Uberlândia (CEUA/UFU-44/2017). Balb-C mice weighing approximately 27 g and nine weeks of age, were used in the experiment. The animals were kept under standard conditions (22 ± 1 °C, humidity 60 ± 5 % and 12 hours light/12 hours dark) and water and ration *ad libitum*. The thirty-two animals used in the experiment were distributed in four treatment groups as shown in Table I. The vehicle used for the treatment of TiO<sub>2</sub>-NCs and PFAC was obtained with 30% lanolin and 70% vaseline.

### Induction and evaluation of wound closure

The experiment was carried in Rede de Biotério e Roedores da Universidade Federal de Uberlândia. Before wound induction, the animals were previously anesthetized with xylazine/ketamine (Syntec) (10:100 mg kg<sup>-1</sup>) intraperitoneally. The animals were trichotomized in the dorsal region and four 5 mm wounds were created with a punch. Images of the wounds on days 0 and 7 days were obtained with a camera (Sony Cybershot 14,1 DSC W320). The wound area was measured with a digital caliper (150 mm-Matrix), after the wound induction (day 0), after 3 days of treatment and after euthanasia (after 7 days of treatment). These measurements were then

**Table I. Distribution and description of groups of animals (untreated and treated).**

Groups	Description	Number of animals
CO	Injured and untreated animals	8
PFAC	Animals injured and treated with an ointment containing 4% PFAC (2% of n-butanol and 2% of ethyl acetate fractions)	8
TiO <sub>2</sub> -NCs	Animals injured and treated with an ointment containing 1% TiO <sub>2</sub> -NCs	8
PFAC +TiO <sub>2</sub> -NCs	Animals injured and treated with a formulated ointment containing PFAC and TiO <sub>2</sub> -NCs associated in previous concentrations	8
	TOTAL	32

used to calculate the percentage of wound closure using the following equations:

Wound area = (smaller diameter /2) \* (larger diameter/2) \* π and area measurement (%) =% wound closure = [1-(Af)/(Af0) X 100], where: Af is the wound area on the evaluated day; Af0 is the initial wound area (Pinto et al. 2016).

### Collection of tissue samples

After 7 days of treatment, the animals were euthanized by deepening anesthetic with 100mg / kg of thiopental (Thiopental®) intraperitoneally. The dorsal skin was removed and 5 mm punch the wounds were obtained. One of the wounds was immediately fixed in metacarn (methanol, acetic acid and chloroform in the ratio of 6: 3: 1 respectively) and subjected to histological processing. The samples destined for biochemical tests (activity of the enzymes myeloperoxidase, n-acetyl-β-D-glucosidase and metalloproteinase-2 activity) were kept in liquid nitrogen and later stored at - 80° C in an ultra-freezer until the moment of the analysis.

### Morphological evaluation

After the fixation of the wound, this was included in paraffin. For each wound included, three sections were obtained with 5 μm thickness in a rotating microtome (Microm / HM-315). One of the cuts was stained with 0.25% Toluidine Blue in MacIlvaine pH 4.0 buffer, another with Gomori Trichrome and last with Sirius Red. These stains were used for the quantification of mast cells, blood vessels and collagen, respectively. For all analyzes, for each slide, ten photomicrographs of different areas were obtained. For the quantification of mast cells and blood vessels, the images were obtained in the Leica Microsystems Inc. type microscope (Wetzlar) with the 40x objective (400x of magnitude) in a coupled camera. For the differentiation and quantification of collagen types I and III,

these photomicrographs were obtained with 20x objective (200X of magnitude), captured in the Nikon eclipse Ti camera, optic camera with polarization filter. All quantifications were performed with the Iagem software (Rasband 2011). For the quantification of mast cells and blood vessels, we used the multiple point tool and for the quantification of collagen, we used the threshold tool. The values were represented by the average as described below:

1 wound per animal = 1 histological slide = 10 different areas

**Average=** total quantification results obtained in the 10 areas / 10 (number of areas evaluated)

### Myeloperoxidase activity

Neutrophil activity can be detected using the myeloperoxidase (MPO) enzyme as a marker (Bradley et al. 1982). The skin sample was homogenized in 2 mL of sodium phosphate buffer, 80 mM at pH = 6. Then, 300 μL of the sample was transferred to microtube and 600 μL of HTAB (Hexadecyltrimethylammonium bromide – Sigma-Aldrich) 0.75% w / v diluted in phosphate buffer pH 6 was added. The samples were sonicated and then centrifuged at 2.700 x g, for 10 minutes at 4°C. The supernatant (200 μL) was used in the enzymatic assay. The reaction followed the following order: 100μL of hydrogen peroxide 0.003 %; 100 μL of TMB (3,3', 5,5' - tetramethylbenzidine - Sigma) at 6.4 mM diluted in DMSO (dimethyl sulfoxide - Merck) placed at the same time. For stop the reaction, 100μL of 4M H<sub>2</sub>SO<sub>4</sub> (sulfuric acid - Merck) was added. Then, 200 μL samples were added in 96-well plate and the spectrophotometric reading was performed at a wavelength of 450nm (E max, Molecular devices). Results were expressed as MPO index (absorbance in optical density/g wet weight of the sample).

### **N-acetyl-β-D-Glucosaminidase activity**

N-acetyl-β-D-glucosaminidase (NAG) is a lysosomal enzyme produced by activated macrophages. This technique is based on the hydrolysis of p-nitrophenyl-N-acetyl-β-D-glucosamine (substrate) by N-acetyl-β-D-glucosaminidase, releasing p-nitrophenol (Bailey 1988). Wound was homogenized in 2.0 mL of saline 0.9% with Triton X-100 (Promega) at 0.1%. Subsequently, the homogenate was centrifuged at 960 x g for 10 minutes at 4°C. Supernatant has been collected and 150 μL of this has been added to 150 μL of citrate/phosphate buffer. For the test, 100 μL/well of diluted (duplicate) samples were added to the 96-well ELISA plate. Then, a volume of 100 μL of the substrate (p-nitrophenyl-n-acetyl-β-D-glucosaminidase-Sigma-Aldrich), diluted in citrate/phosphate buffer, pH 4.5, was added and incubated at 37°C for 30 minutes. A volume of 100 μL of 0.2 M glycine buffer, pH 10.6 was added in the samples and to the curve. The absorbance was measured by spectrophotometry at a wavelength of 400 nm (E max, Molecular devices). The NAG activity in the sample of the sample was calculated from a standard curve of p-nitrophenol evaluated in parallel. The results of the readings were expressed in nmol/mg wet weight of the sample).

### **Activity of metalloproteinase 2 (MMP-2) by the zymography method**

Gelatinolytic activity of metalloproteinase 2 (MMP-2) was assessed by the zymography method. Protein quantification was obtained using the Bradford method (Bradford 1976) and 25 μg of sample proteins was applied to the 10% SDS-PAGE gel (sodium polyacrylamide / sodium dodecyl electrophoresis) with 0.4% gelatine (Sigma-Aldrich). This test was carried out with samples of 3 animals from each group in triplicate. After electrophoresis, the

gel was washed with 25% Triton X 100 buffer and incubated for 18 hours at 37 ° C with the incubation buffer (pH 7.4; 50 mM Tris - HCl, 10 mM ZnCl<sub>2</sub>, 10 mM ZnCl<sub>2</sub>, 0.1 M NaCl and protease inhibitor). Gel was stained with 0.5% comassie blue for 2 h and then bleached with bleach solution (methanol / water / acetic acid in the ratio of 6: 3: 1, respectively) until the bands were visualized (MMP2 activity). Gels were digitized and the activity of MMP-2 was evaluated by band densitometry with the software Image J.

### **Statistical analysis**

Statistics were performed showing the mean and standard error. All numerical data were tested for normal distribution using the Kolmogorov-Smirnov test. The one-way analysis of variance (ANOVA) and Bonferroni post-test were performed for multiple comparisons between all data. Differences between error standards were considered significant when p values were <0.05. The statistical evaluation and graphs were performed using the GraphPad Prism software, version 8.0.

## **RESULTS**

### **Characterization of TiO<sub>2</sub> Nanocrystals**

The analysis of high-resolution transmission electron microscopy (HRTEM), X-ray diffraction (XRD) and Raman spectroscopy confirmed the formation of TiO<sub>2</sub> NCs and their characteristics of size, crystalline phase and percentage of these phases (Figure 1).

Figure 1a shows the HRTEM images, with average size of TiO<sub>2</sub>-NCs around 78 nm. The lattice spacing (d) of TiO<sub>2</sub>-NCs is 0.352 nm corresponding to d<sub>110</sub> spacing of rutile TiO<sub>2</sub> crystal. It is also observed the formation of other forms of nanocrystals providing indications of different phases. XRD patterns of the sample subjected to thermal annealing at 800°C/h, where standard

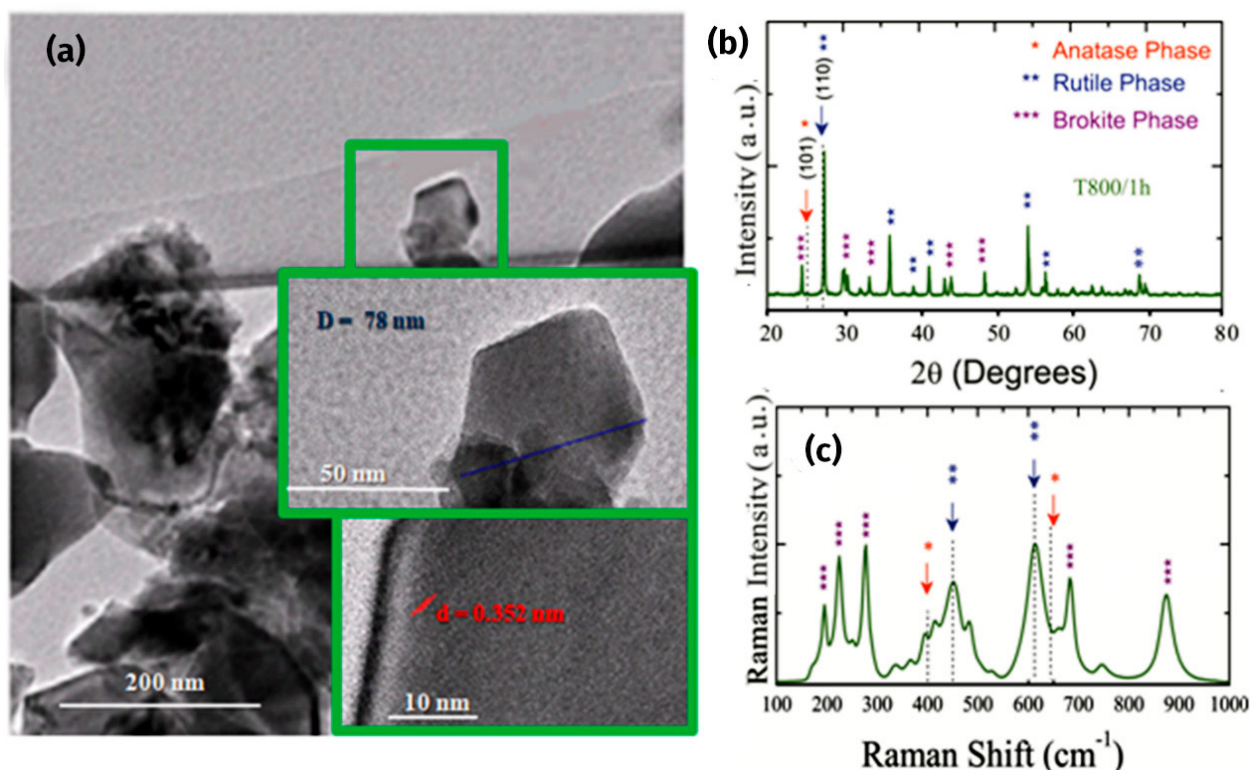


**Figure 1. Characterization of TiO<sub>2</sub>-NCs.** (a) HRTEM images, (b) XRD patterns, and (c) Raman spectrum of the TiO<sub>2</sub>-NCs thermal annealing at 800° C/h, where standard cards represented by asterisks of the crystalline phase.

cards represented by asterisks of the crystalline phase in the XRD patterns (Figure 1b). In the XRD pattern of the TiO<sub>2</sub>-NCs observed, the presence of Bragg diffraction peaks characteristic of anatase (JCPDS card no. 21-1272), brookite (JCPDS card no. 29-1360) and predominant rutile (JCPDS card no. 21-1276) phase. The percentage of anatase, brookite, and rutile phases is 1%, 35%, and 64 %, respectively.

Raman spectrum of TiO<sub>2</sub>-NCs with thermal annealing at 800°C/ h was normalized to the peak of higher intensity as shown in Figure 1c. Raman spectrum exhibited the characteristic Raman bands of vibrations of anatase, rutile and brookite phases (Balachandran & Eror 1982, Castrejón-Sánchez et al. 2014). The presence of the bands of the brookite phase was observed in the Raman spectrum, as confirmed in the XRD results. The absence of impurity peaks reinforces evidence that these TiO<sub>2</sub>-NCs are of high purity.

### TiO<sub>2</sub>-NCs and PFAC accelerates the closure of skin wounds

The wound closure of animals treated with PFAC and TiO<sub>2</sub>-NCs was measured and the healing effect of these treatments is shown in Figure 2a. Macroscopic images of healing were also obtained after wound induction and at the end of each treatment (Figure 2b). After 3 days of treatment, wounds treated with TiO<sub>2</sub>-NCs showed an accelerated closure of 41.4% when compared to the CO group and 57.1% greater in relation to the healing observed in the PFAC group. In the same period, treatment with PFAC + TiO<sub>2</sub>-NCs showed a delay in wound closure by 54.2%, 10% and 58.65% in relation to all other groups, CO, PFAC and TiO<sub>2</sub>, respectively (Figure 2a). After seven days of treatment, an accelerated closure of 25.1% was observed in wounds treated with PFAC in relation to the CO group. During this period, there was again a

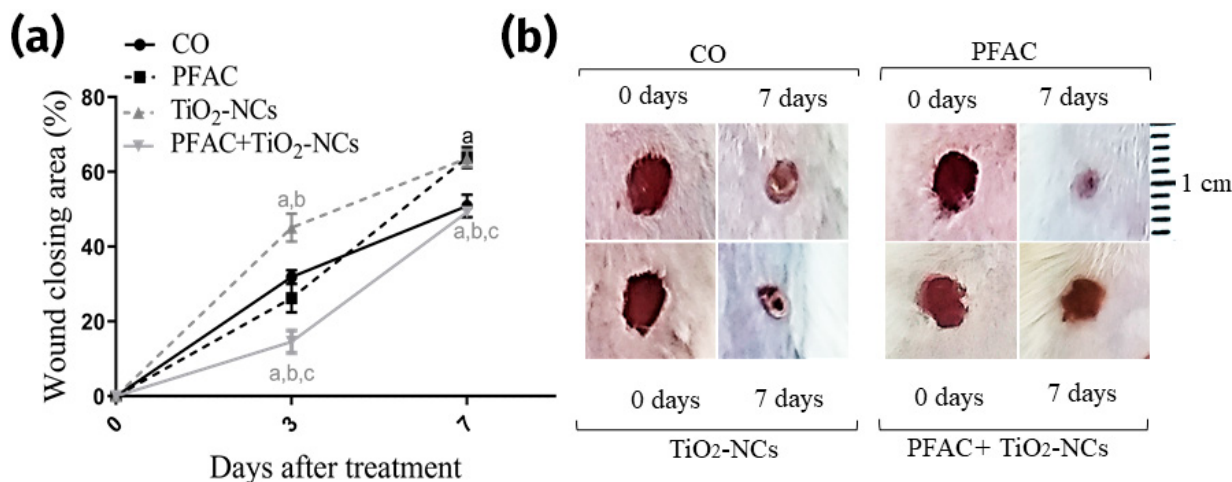


**Figure 2.** Percentage of wound closure in area. (a) Wound closure after 3 and 7 days of treatment in untreated (CO) and treated groups (PFAC, TiO<sub>2</sub>-NCs, and PFAC+TiO<sub>2</sub>-NCs). (a) Indicates statistical difference considering  $p < 0.05$  when compared with CO (b) PFAC and (c) TiO<sub>2</sub>-NCs groups, assessed by One-Way ANOVA and Bonferroni test. Values are mean  $\pm$  SEM (n=8). (b) Macroscopic images of the wound after induction (day 0) and after 7 days of treatment.

delay in the closure of wounds treated with PFAC + TiO<sub>2</sub>-NCs with closure similar to the CO group and lower by 28.8% and 26.6% in relation to the PFAC and TiO<sub>2</sub>-NCs groups, respectively (Figure 2a and Figure 2b).

### The treatment of wounds with TiO<sub>2</sub>-NCs and PFAC+TiO<sub>2</sub>-NCs have opposite effects on the activities of NAG and MPO

Wounds treated with PFAC and TiO<sub>2</sub>-NCs showed MPO activity of 64.1% and 86.6% less, respectively, than the activity of this enzyme and untreated wounds (CO group). PFAC+TiO<sub>2</sub>-NCs activity was 85.9% higher than MPO activity in wounds in the TiO<sub>2</sub>-NCs group (Figure 3a). There was no statistical difference on NAG activity between treated and untreated groups (CO group). Otherwise, wounds treated with TiO<sub>2</sub>-NCs showed NAG activity increased by 59.7% in relation to the PFAC group and by 48.1% in relation to the PFAC + TiO<sub>2</sub>-NCs group (Figure 3b).

### Treatment with PFAC+TiO<sub>2</sub>-NCs increases the number of mast cells in the wound area

Wounds from animals treated with PFAC+TiO<sub>2</sub>-NCs showed a mean (0.32) of mast cells in the wound area compared to the values found for groups CO (0.03) and PFAC (0.04) (Figure 4a). There was no statistical difference on the mean number of mast cells in the wound area between the other groups evaluated. Photomicrographs stained with Toluidine Blue representing the mast cell quantification results are shown in Figure 4b. The mean blood vessels in wound samples were not statistically different between the groups evaluated (Figure 4c). In Figure 4d, blood vessels in the wound area were also demonstrated in photomicrographs stained with Gomori Trichomic.

### Treatments with PFAC and TiO<sub>2</sub>-NCs increase the deposition of type I and III collagen, while wounds treated with PFAC+TiO<sub>2</sub>-NCs have a predominance of type III collagen

Wounds treated with PFAC and TiO<sub>2</sub>-NCs showed an increase in both types of collagen, type I and III. The quantification of these fibers (Figures 5a and 5b) was performed in photomicrographs

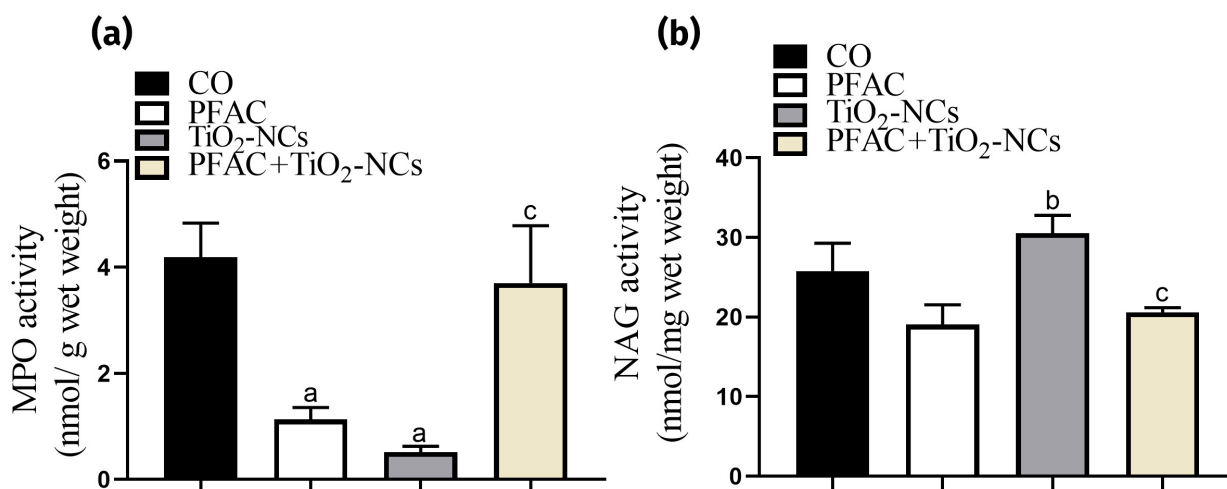


**Figure 3.** Activity of the enzymes myeloperoxidase (MPO) and N-acetyl- $\beta$ -D-glucosamine (NAG) on the skin of the wound. (a) Activity of MPO and (b) NAG enzymes in wound of untreated groups (CO) and the treated groups (PFAC, TiO<sub>2</sub>-NCs and PFAC+TiO<sub>2</sub>-NCs). (a) Indicates statistical difference considering  $p < 0.05$  when compared with CO, (b) PFAC and (c) TiO<sub>2</sub>-NCs groups assessed by One-Way ANOVA and Bonferroni test. Values are mean  $\pm$  SEM (n=8).

obtained with a polarization filter on slides stained with Sirius Red (Figure 5d). Wounds increased type I collagen fibers by 75.8% and 55.7% when treated with PFAC and TiO<sub>2</sub>-NCs, respectively. The increase was also observed in the same groups for type III collagen, with an increase of 68% in PFAC and 50.2% in TiO<sub>2</sub>-NCs. All of these results were obtained after comparison with the CO group. (Figure 5b). When compared with TiO<sub>2</sub>-NCs group, wounds treated with PFAC+TiO<sub>2</sub>-NCs showed a 33.8% reduction in type I collagen fibers (Figure 5a). The ratio between the two types of collagen was calculated. In the graph presented in figure 5c, it is possible to observe that wounds treated with PFAC+TiO<sub>2</sub>-NCs showed a predominance of type III collagen in relation to the presence of type I fibers. This ratio was higher in 13.1% and 13.5% in wounds treated with PFAC+TiO<sub>2</sub>-NCs compared to the PFAC and TiO<sub>2</sub>-NCs groups, respectively (Figure 5d).

### TiO<sub>2</sub>-NCs and PFAC+TiO<sub>2</sub>-NCs increase MMP-2 activity in wounds

The bands resulting from MMP-2 activity on zymography gel (Figure 6b) were quantified in the software J and the results are shown in Figure 6a. MMP-2 activity was increased by 129.5% and 94.1% when the wounds were treated with TiO<sub>2</sub>-NCs and PFAC+TiO<sub>2</sub>-NCs, respectively, when compared to the CO group. Otherwise, wounds treated with PFAC showed MMP-2 activity similar to that found for untreated wounds (group CO) (Figure 6a). Considering the treated groups, there was a 62.3% increase in MMP-2 activity in wounds treated with TiO<sub>2</sub>-NCs compared to the PFAC group (Figure 6a).

## DISCUSSION

The aim of this study was to evaluate the biological effect of treating wounds with TiO<sub>2</sub>-NCs and PFAC individually and in combination (PFAC + TiO<sub>2</sub>-NCs). These nanocrystals are 78 nm in size and consist of the rutile (64%), brookite (35%) and anatase (1%) phases. TiO<sub>2</sub>-NCs used in our study were previously evaluated and proved

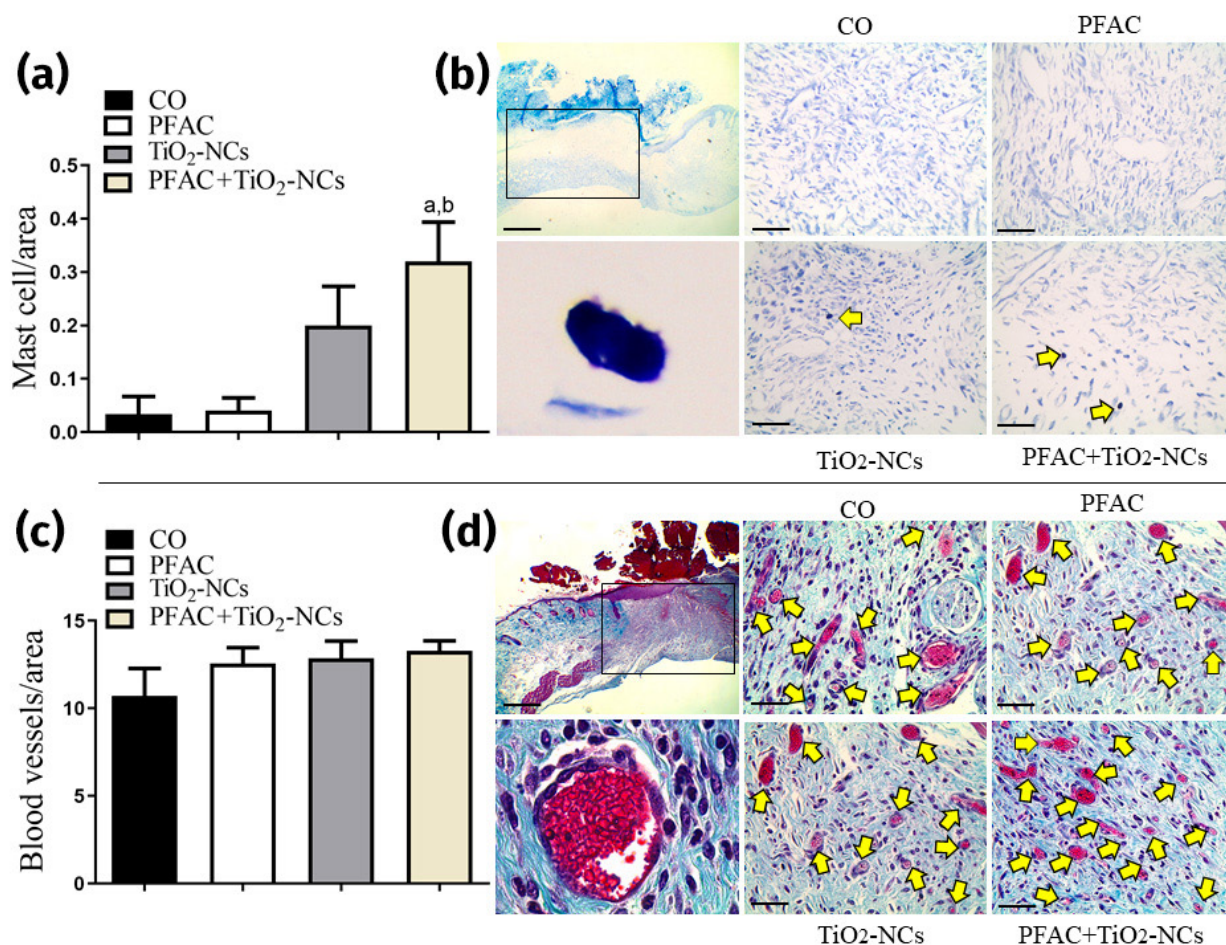


**Figure 4.** Average number of mast cells and blood vessels in the wound area. (a) Mean mast cells in wound area on slides stained with Toluidine Blue and (b) mean blood vessels per wound area on slides stained with Gomori Trichomic of untreated (CO) and treated groups (PFAC, TiO<sub>2</sub>-NCs, and PFAC+TiO<sub>2</sub>-NCs). (a) Indicates statistical difference considering  $p < 0.05$  in relation to the CO and (b) PFAC groups, assessed by One-Way ANOVA and Bonferroni test. Values are mean  $\pm$  SEM (n=8). Photomicrographs show the delimitation of the wound area which quantified mast cells (b) and blood vessels (d) with scale bar indicating 500  $\mu$ m, these images also demonstrate an enlarged image of a mast cell (b) and blood vessel (d); In the following images the mast cells (b) and blood vessels (d) in the wound area are represented in micrographs identified by arrows (scale bar of 50  $\mu$ m).

to be highly safe for application in biological tests and therapeutic indications (Reis et al. 2016). Other factors that justify its use are the biocompatibility of these nanomaterials (Otero-González et al. 2013) and the characteristic stability of the rutile / brookite mixture (Schilling et al. 2010). In addition, treatment with TiO<sub>2</sub>-NCs with a predominance of the rutile phase has greater cell viability (Duarte et al. 2020).

The wound healing process is subdivided into four phases, which occur in an overlapping

manner: hemostasis, inflammation, proliferation, and tissue remodeling (Gosain & DiPietro 2004). There are many factors that can affect healing. These interfere with one or more phases in this process, thus causing improper or impaired tissue repair. The events that occur in each of these phases are well known, and the prolonged inflammation, as well as collagen synthesis and impaired angiogenesis can delay the healing process (Guo & DiPietro 2010). The activity of and MMP9 play a key role in cell migration,

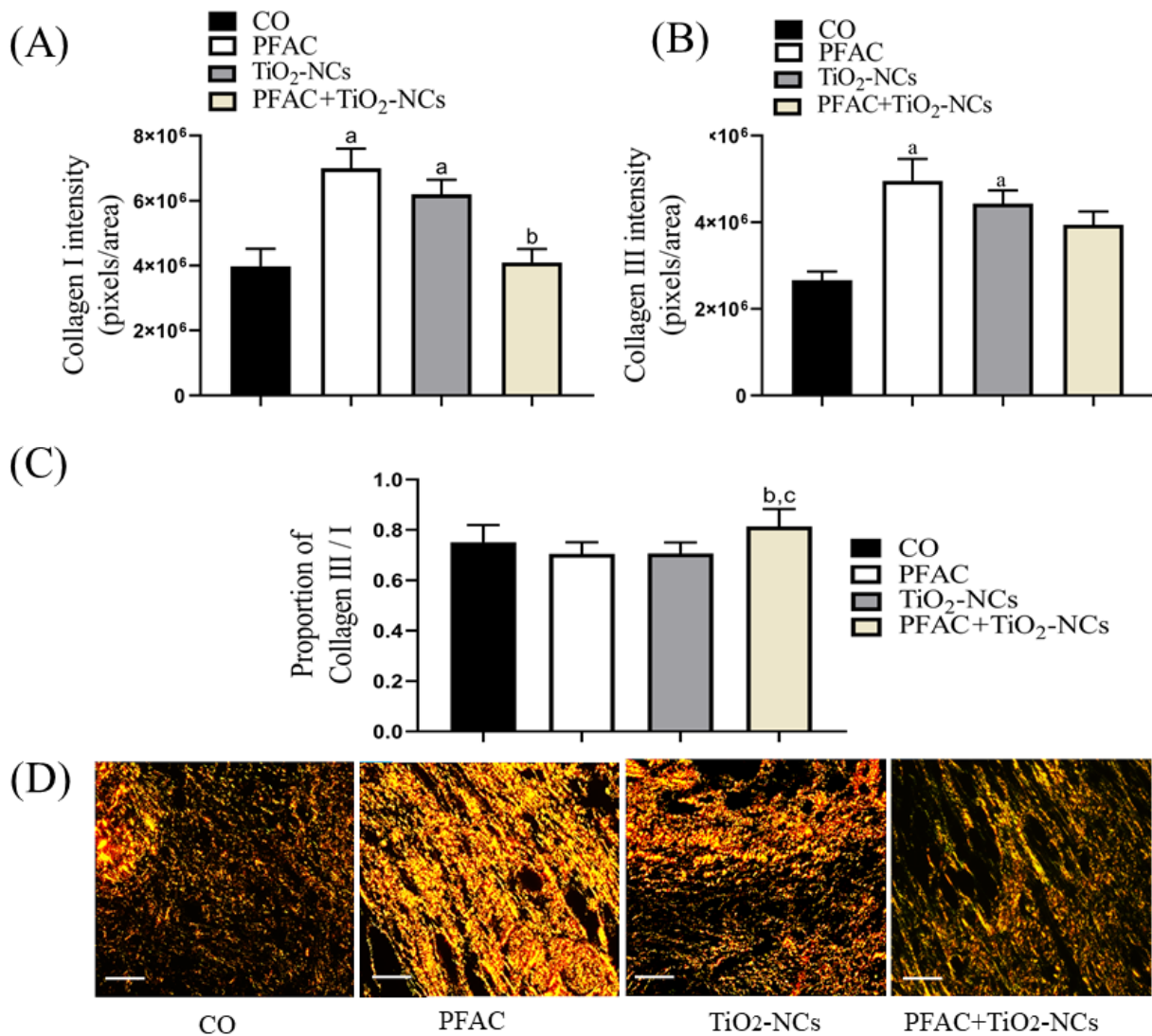


**Figure 5.** Quantification of type I and III collagen in treated (PFAC, TiO<sub>2</sub>-NCs and PFAC + TiO<sub>2</sub>-NCs) and untreated (CO) wounds. Quantification of types I (a) and III (b) collagen and (C) ratio between collagen III/I in photomicrographs stained with Sirius Red. (a) indicates statistical difference considering  $p < 0.05$  when compared with untreated animals (group CO), (b) with PFAC and (c) TiO<sub>2</sub>-NCs groups, assessed by One-Way ANOVA and Bonferroni test. Values are mean  $\pm$  SEM (n=8). Photomicrographs (d) demonstrating type I collagen in red and type III collagen in green, in orange / yellow is the overlap of the two types of collagen (types I and III). In these images the bar represents 50  $\mu$ m.

especially keratinocytes to promote wound re-epithelization (Caley et al. 2015). Together, these parameters contribute to quality and a shorter wound closure time, therefore, being evaluated in our study. This is the first study to evaluate the effect of the treatment of wounds with TiO<sub>2</sub>-NCs on the activity of neutrophils, macrophages and MMP-2 and collagen deposition in the

extracellular matrix. Otherwise, in our previous study, was demonstrated the anti-inflammatory, pro-fibrogenic and healing property of PFAC. This treatment had no effect on angiogenesis (De Moura et al. 2019) and data on MMP-2 activity are not available.

Wounds treated with TiO<sub>2</sub>-NCs and PFAC accelerated wound closure. This data reinforces

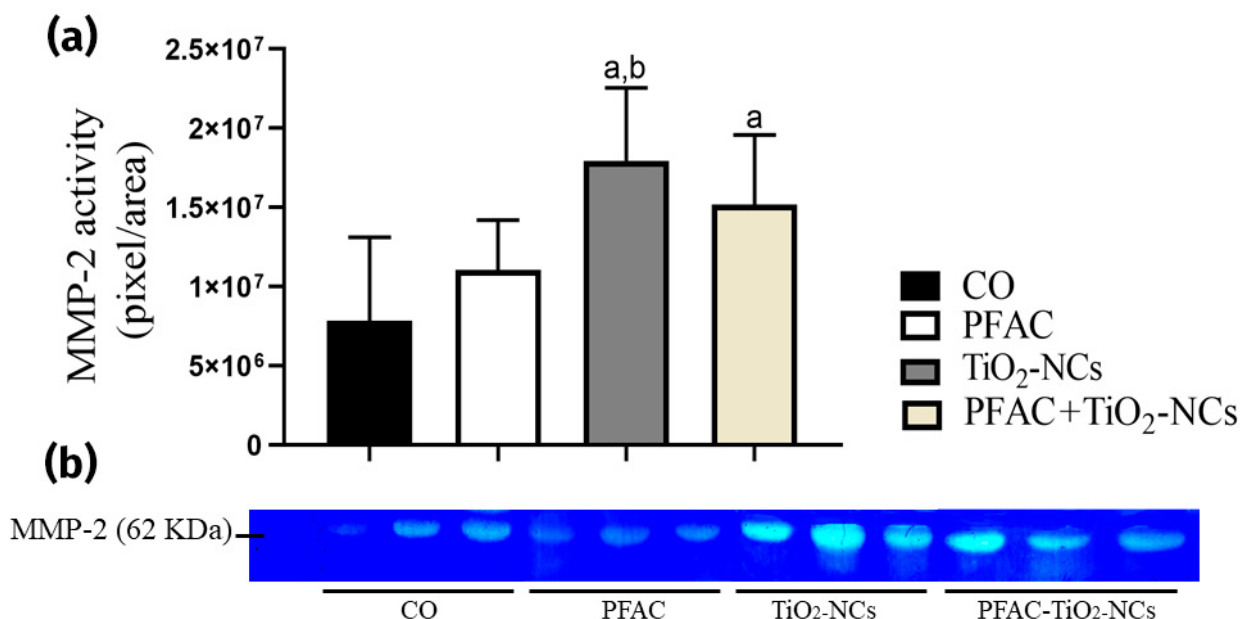


**Figure 6.** Quantification of MMP-2 activity in skin wounds by the zymogram method. (a) Densitometry quantification of MMP-2 activity on 10% polyacrylamide gel containing 0.4% gelatin of the untreated groups (CO) and the treated groups (PFAC, TiO<sub>2</sub>-NCs and TiO<sub>2</sub>-NCs- PFAC). (a) indicates statistical difference considering  $p < 0.05$  when compared with CO group and (b) PFAC groups, assessed by One-Way ANOVA and Bonferroni test. Values are mean  $\pm$  SEM (n=8) (b) Zymography gel with bands (MMP-2 activity) in the control and treated group.

the healing property of TiO<sub>2</sub>-NPs and PFAC demonstrated in other studies (De Moura et al. 2019, Nikpasand & Parvizi 2019, Seisenbaeva et al. 2017, Sivaranjani & Philominathan 2016). Treatment with TiO<sub>2</sub>-NPs also improves healing in burn models of 2nd and 4th degree burns (Seisenbaeva et al. 2017) and PFAC analysis by HPLC (high performance liquid chromatography) demonstrated the present of polyphenols such as epicatechin, proanthocyanidin, kaempferol and quercetin (Justino et al. 2016), which contributed to accelerating the healing process (De Moura et al. 2019).

The exaggerated inflammatory response is one of the factors that compromise the healing process (Bjarnsholt et al. 2008, Guo & Dipietro 2010). Thus, in our study, suggest that the reduction of neutrophil activity in wounds treated with TiO<sub>2</sub>-NCS and PFAC may have contributed to the favorable results for wound closure. The anti-inflammatory activity of polyphenols in the

peel of *A. crassiflora* fruit was also evaluated in mouse paw edema. In this study, as in our wound assessment, a reduction in neutrophil activity was observed using the MPO method. In addition, was demonstrated that polyphenols present in the peel of this fruit were able to reduce the production of nitric oxide and the pro-inflammatory cytokine interleukin-6 (IL-6) derived from macrophages stimulated by LPS (Justino et al. 2019).

Considering the treatment with TiO<sub>2</sub>-NCs. The reduction in neutrophil activity may be associated with the property of TiO<sub>2</sub>-NPs in reducing leukocyte infiltration in the wound area (Agarwal et al. 2019). The reduction in neutrophil activity observed in wounds treated with TiO<sub>2</sub>-NCs was also consistent with the *in vitro* study, in which TiO<sub>2</sub>-NPs induced the maximum influx of neutrophils in the initial period of the inflammatory response, after 3-9 hours of treatment, being subsequently (12-24 hours)

progressively reduced (Gonçalves & Girard 2011). The reduction on neutrophil activity in wounds treated with TiO<sub>2</sub>-NCs and PFAC as individual treatments is essential, because although the participation of neutrophils is crucial for the resolution of the inflammatory process, when these cells remain in the wound, can impair the healing process (Guo & Dipietro 2010). This is because neutrophils release reactive oxygen species (ROS) and proteases in excess, enough to damage the local tissue, impairing the migration of cells through the extracellular matrix and compromising the progression and quality of the repair (Guo & Dipietro 2010).

In addition to the treatment with TiO<sub>2</sub>-NCs, we evaluated the effect of a formulation containing a mix of TiO<sub>2</sub>-NCs and PFAC. TiO<sub>2</sub>-NPs have a strong interaction with polyphenols that is demonstrated and proven even by simple preparation methods. This interaction can be seen after the homogenization of TiO<sub>2</sub>-NPs in double-distilled water and even after simple dilutions such as humidification of TiO<sub>2</sub>-NPs with ethanol and subsequent addition of the flavonoids and stirring for 24 hours (Cao et al. 2016, Khan et al. 2017). The interactions between TiO<sub>2</sub> and polyphenols are confirmed by UV-Vis spectrometry and Raman spectrometry (Cao et al. 2016). Formulation to treat wounds containing nanoparticles and plant compounds has been evaluated with other nanoparticles (Krychowiak et al. 2014), but there are no studies that evaluate the effect of these formulations containing TiO<sub>2</sub>-NCs. Although TiO<sub>2</sub>-NCs and PFAC have healing and anti-inflammatory characteristics, this result was not observed for the combined treatments (PFAC+TiO<sub>2</sub>-NCs). The increased activity of neutrophils and reduced macrophages in wounds treated with PFAC + TiO<sub>2</sub>-NCs in relation to the TiO<sub>2</sub>-NCs group, indicate a delay in healing (Ortega-Gómez et al. 2013). This is because after performing

its function, neutrophils, in normal healing, are reduced by apoptosis and phagocytosed by macrophages, an essential event for the resolution of inflammation (Ortega-Gómez et al. 2013). In the PFAC+TiO<sub>2</sub>-NCs group, this harmful modulation of inflammatory cell activity may have contributed to the delayed wound closure result.

The properties of phenolic compounds are largely affected by the electronic nature of the substituents and their position in the aromatic ring. These modifications can occur via TiO<sub>2</sub> catalysis (Parra et al. 2003). Thus, we suggest that the effects obtained through the isolated treatments were not observed in wounds treated with PFAC+TiO<sub>2</sub>-NCs due to the interaction between the OH groups of polyphenols and TiO<sub>2</sub>-NCs. The polyphenols found in PFAC have OH groups in different positions, which influences the absence or presence of these interactions. For example, polyphenols found in citrus fruits interact with TiO<sub>2</sub>-NPs with groups 3'-OH and 4'-OH in ring B, forming a charge transfer complex, while polyphenols with available groups C=O in ring C and 5'-OH in the ring did not bind with TiO<sub>2</sub>-NPs (Cao et al. 2016). These interactions can increase or decrease biological activities. It is known that the interaction of TiO<sub>2</sub>-NPs with catechin results in increased antioxidant activity, while their interaction with quercetin reduces this activity. In addition, the ability of TiO<sub>2</sub>-NPs to promote lipoperoxidation is reduced when TiO<sub>2</sub>-NPs interacts with quercetin and catechin compared to the effect of TiO<sub>2</sub>-NPs alone (Yu et al. 2019). Through X-Ray diffraction and scanning electron microscopy techniques it has been proposed that modifications in TiO<sub>2</sub>-NPs promoted by phenols result in changes in the degree of crystallinity without changes in the size of the nanoparticle (Yu et al. 2019).

This modulatory capacity of biological activities was also reflected in the mast cell

quantification. Mast cells play a fundamental role in the stages of inflammation, proliferation and remodeling of the wound healing process (Kennelly et al. 2011). The number of these cells was increased in wounds treated with PFAC + TiO<sub>2</sub>-NCs compared with CO and PFAC groups, and considered statistically similar to treatment with TiO<sub>2</sub>-NCs. Polyphenols found in PFAC have been shown to have a negative effect on mast cell activity. The proposed mechanism for this action is due to the ability of these compounds to inhibit immunoglobulin E (IgE-mediated histamine release), in addition to reducing gene expression and the production of pro-inflammatory cytokines (Komi et al. 2019). From this, we can suggest that the interaction of these polyphenols with TiO<sub>2</sub>-NCS may be able to also modulate this inhibitory activity, resulting in the increase of mast cells in the injured area in PFAC+TiO<sub>2</sub>-NCs group. The increase in mast cells in the injured area in this group may be associated with an increase in neutrophil activity. This is because mast cells are cells that release mediators such as tumor necrosis factor alpha (TNF- $\alpha$ ), macrophage inflammatory protein-2 (MIP-2), and interleukin 8 (IL-8) that have the ability to recruit neutrophils during wound repair (Egozi et al. 2003).

During the proliferation phase, marked by the formation of a granulation tissue, the processes of angiogenesis and fibrogenesis are accentuated. The angiogenesis plays an important role in tissue regeneration because blood vessels supply oxygen and nutrients to growing cells and tissues (Saghiri et al. 2015a, 2015b). As in our previous study, PFAC was unable to modulate angiogenic activity in treated wounds (De Moura et al. 2019). Changes in angiogenic capacity were also not observed in wounds treated with TiO<sub>2</sub>-NCs and PFAC+TiO<sub>2</sub>-NCs, demonstrating that the biological activity

of these different treatments was not influenced by the interactions.

The pro-fibrogenic activity of PFAC and TiO<sub>2</sub>-NCs individually, was also not maintained in the associated treatment (PFAC+TiO<sub>2</sub>-NCs). In this study we demonstrated that both types of collagen (collagen I and III) were increased in wounds treated with PFAC and TiO<sub>2</sub>-NCs. This pro-fibrogenic activity of PFAC was demonstrated previously in our previous study (De Moura et al. 2019). However, in this study, we demonstrate for the first time the activity of TiO<sub>2</sub>-NCs in stimulating the synthesis of type I and III collagen on skin wounds. Wounds treated with PFAC+TiO<sub>2</sub>-NCs do not show an increase in collagen of both types (type I and III), the extracellular matrix of wounds in this group showed the characteristic of an immature extracellular matrix (McKelvey et al. 2014, Xue & Jackson 2015), with a predominance of type III collagen in relation to type I collagen when compared to individual treatments (PFAC and TiO<sub>2</sub>-NCs). This result may have contributed to the delay in wound closure in this group. The collagen composition of non-damaged adult skin is approximately 80% of type I collagen and 10% of type III collagen. However, during a proliferation phase, there is a predominance of type III collagen that is deposited on an extracellular matrix (Wilkinson & Hardman 2020). As healing progresses, this immature collagen (type III collagen) is progressively replaced by type I collagen, intensifying the tensile strength of the scar in formation (Wilkinson & Hardman 2020). In view of our results, we suggest that different from the immature matrix characteristic observed in wounds of the PFAC+TiO<sub>2</sub>-NCs group, treatments with PFAC and TiO<sub>2</sub>-NCs accelerated this process, which may have contributed to a skin with greater tensile strength.

Unlike this pattern, MMP-2 activity was increased in wounds treated with TiO<sub>2</sub>-NCs and

PFAC+TiO<sub>2</sub>-NCs, but not in wounds treated only with PFAC. MMPs play a crucial role in all stages of wound healing by modifying the wound matrix, allowing for cell migration and tissue remodeling (Caley et al. 2015). These metalloproteinases can be produced by both neutrophils (Wilgus & Wulff 2014) and fibroblasts (Martins et al. 2013). In wounds treated with TiO<sub>2</sub>-NCs, fibroblasts play a greater role in the production of MMP-2. This is because these wounds aggregate collagen, a protein synthesized mainly by these cells, at the same time as reduced neutrophil activity. The increase in MMP-2 activity in wounds treated with TiO<sub>2</sub>-NCs may have contributed to accelerated closure. This is because studies show that MMP-2 can cleave the gamma-2 chain of laminin-322 forming a fragment that has a role similar to the epidermal growth factor (EGF). This fragment, binds to the EGF receptor, being able to trigger the migration of keratinocytes to the wounded matrix, contributes to the wound closure (Caley et al. 2015).

Differently from that observed for wounds treated with TiO<sub>2</sub>-NCs, in wounds of TiO<sub>2</sub>-NCS + PFAC group, neutrophils may have a greater contribution in increasing MMP-2 activity. Although MMP-2 is essential for the repair of wounds, when these are accompanied by an increase in the activity of inflammatory cells, these tend impairing healing. Thus, the increase in MMP-2 accompanied by the increase in neutrophils, as observed in wounds treated with PFAC+ TiO<sub>2</sub>-NCs is a profile found in chronic wounds (Guo & Dipietro 2010, Wilgus & Wulff 2014). These wounds are found in a prolonged inflammation, stage with less participation of keratinocytes and fibroblasts. In this scenario, MMP-2 tends to damage a newly formed extracellular matrix, which impairs the migration of keratinocytes and fibroblasts, causing a delay in the closure of these wounds.

## CONCLUSIONS

The treatment with PFAC+ TiO<sub>2</sub>-NCs did not enhance the results found for wounds treated with PFAC and TiO<sub>2</sub>-NCs individually. The associated treatment resulted in marked differences in wound closure, inflammatory cell activity, MMP-2 activity and collagen on extracellular matrix. TiO<sub>2</sub>-NCs and PFAC showed promising results for wound healing, while wounds treated with PFAC+TiO<sub>2</sub>-NCs presented an impaired healing process. Otherwise, none of the treatments had an effect on angiogenesis in the evaluated time. The interaction between the hydroxyl groups of polyphenols present in PFAC with TiO<sub>2</sub>-NCs may have contributed to these results and should be better evaluated.

## Acknowledgments

This study was financed by the Coordenação de Aperfeiçoamento de Pessoal de Nível Superior - Brasil (CAPES) - Finance Code 001, Fundação de Amparo à Pesquisa do Estado de Minas Gerais FAPEMIG) and Conselho Nacional de Desenvolvimento Científico e Tecnológico (CNPq) and the National Institute of Science and Technology in Theranostics and Nanobiotechnology—INCT-TeraNano (CNPq / CAPES / FAPEMIG, CNPq-465669 / 2014- 0 and FAPEMIG-CBB-APQ-03613-17). FSE receives scholarship grants from FAPEMIG (PPM-00503-18) and CNPq (PQ - Research productivity, process no. 312812/2021-3).

## REFERENCES

- AGARWAL H, NAKARA A & SHANMUGAM VK. 2019. Anti-inflammatory mechanism of various metal and metal oxide nanoparticles synthesized using plant extracts: A review. *Biomed Pharmacother* 109: 2561-2572.
- ARCHANA D, SINGH BK, DUTTA J & DUTTA PK. 2013. *In vivo* evaluation of chitosan-PVP-titanium dioxide nanocomposite as wound dressing material. *Carbohydr Polym* 95: 530-539.
- BAILEY PJ. 1988. Sponge Implants as Models. *Methods Enzymol* 162: 327-334.
- BALACHANDRAN U & EROR NG. 1982. Raman spectra of titanium dioxide. *J. Solid State Chem* 42: 276-282.

- BJARNSHOLT T, KIRKETERP-MØLLER K, JENSEN PØ, MADSEN KG, PHIPPS R, KROGFELT K, HØIBY N & GIVSKOV M. 2008. Why chronic wounds will not heal: A novel hypothesis. *Wound Repair Regen* 16: 2-10.
- BRADFORD M. 1976. *Snakes of India: The Field Guide* 72: 248-254.
- BRADLEY PP, PRIEBAT DA, CHRISTENSEN RD & ROTHSTEIN G. 1982. Measurement of cutaneous inflammation: Estimation of neutrophil content with an enzyme marker. *J Invest Dermatol* 78: 206-209.
- CALEY MP, MARTINS VLC & O'TOOLE EA. 2015. Metalloproteinases and Wound Healing. *Adv Wound Care* 4: 225-234.
- CAO X, MA C, GAO Z, ZHENG J, HE L, MCCLEMENTS DJ & XIAO H. 2016. Characterization of the Interactions between Titanium Dioxide Nanoparticles and Polymethoxyflavones Using Surface-Enhanced Raman Spectroscopy. *J Agric Food Chem* 64: 9436-9441.
- CASTREJÓN-SÁNCHEZ VH, CAMPS E & CAMACHO-LÓPEZ M. 2014. Quantification of phase content in TiO<sub>2</sub> thin films by Raman spectroscopy. *Superf Vacio* 27: 88-92.
- DE MOURA FBR, JUSTINO AB, FERREIRA BA, ESPINDOLA FS, ARAÚJO FDA & TOMIOSSO TC. 2019. Pro-Fibrogenic and Anti-Inflammatory Potential of a Polyphenol-Enriched Fraction from *Annona crassiflora* in Skin Repair. *Planta Med* 85: 570-577.
- DUARTE CA ET AL. 2020. Characterization of Crystalline Phase of TiO<sub>2</sub>. *Materials (Basel)* 13: 4071.
- EGOZI EI, FERREIRA AM, BURNS AL, GAMELLI RL & DIPIETRO LA. 2003. Mast cells modulate the inflammatory but not the proliferative response in healing wounds. *Wound Repair Regen* 11: 46-54.
- EKOR M. 2014. The growing use of herbal medicines: Issues relating to adverse reactions and challenges in monitoring safety. *Front Neurol* 4: 1-10.
- FAN X, CHEN K, HE X, LI N, HUANG J, TANG K, LI Y & WANG F. 2016. Nano-TiO<sub>2</sub>/collagen-chitosan porous scaffold for wound repairing. *Int J Biol Macromol* 91: 15-22.
- GEORGESCU M, MARINAS O, POPA M, STAN T, LAZAR V, BERTEȘTEANU SV & CHIFIRIUC MC. 2016. Natural compounds for wound healing. In: *Worldwide Wound Healing - Innovation in Natural and Conventional Methods*. Croatia: Intech, p. 61-89.
- GONÇALVES DM & GIRARD D. 2011. Titanium dioxide (TiO<sub>2</sub>) nanoparticles induce neutrophil influx and local production of several pro-inflammatory mediators *in vivo*. *Int Immunopharmacol* 11: 1109-1115.
- GOSAIN A & DIPIETRO LA. 2004. Aging and Wound Healing. *World J Sur* 28: 321-326.
- GUO S & DIPIETRO LA. 2010. Factors Affecting Wound Healing 89: 219-229.
- HAUGEN HJ & LYGSTADAAS SP. 2016. Antibacterial effects of titanium dioxide in wounds. *Wound Healing Biomaterials* 2: 439-450.
- JUSTINO AB ET AL. 2019. Protective effects of a polyphenol-enriched fraction of the fruit peel of *Annona crassiflora* Mart. on acute and persistent inflammatory pain. *Inflammopharmacology* 2019: 1-13.
- JUSTINO AB ET AL. 2016. Peel of araticum fruit (*Annona crassiflora* Mart.) as a source of antioxidant compounds with α-amylase, α-glucosidase and glycation inhibitory activities. *Bioorg Chem* 69: 167-182.
- KENNELLYR, B CONNEELY J, BOUCHIER-HAYES D & C WINTER D. 2011. Mast Cells in Tissue Healing: From Skin to the Gastrointestinal Tract. *Curr Pharm Des* 17: 3772-3775.
- KHAN MA, WALLACE WT, ISLAM SZ, NAGPURE S, STRZALKA J, LITTLETON JM, RANKIN SE & KNUTSON BL. 2017. Adsorption and Recovery of Polyphenolic Flavonoids Using TiO<sub>2</sub>-Functionalized Mesoporous Silica Nanoparticles. *ACS Appl Mater Interfaces* 9: 32114-32125.
- KOMI DEA, KHOMTCHOUK K & MARIA PLS. 2019. A Review of the Contribution of Mast Cells in Wound Healing: Involved Molecular and Cellular Mechanisms. *Clin Rev Allergy Immunol* 2019: 1-15.
- KRYCHOWIAK M, GRINHOLCM, BANASIUKR, KRAUZE-BARANOWSKA M, GŁÓD D, KAWIAK A & KRÓLICKA A. 2014. Combination of silver nanoparticles and *Drosera binata* extract as a possible alternative for antibiotic treatment of burn wound infections caused by resistant *Staphylococcus aureus*. *PLoS One* 9: 1-20.
- LEU JG, CHEN SA, CHEN HM, WU WM, HUNG CF, YAO Y, DER TU CS & LIANG YJ. 2012. The effects of gold nanoparticles in wound healing with antioxidant epigallocatechin gallate and α-lipoic acid. *Nanomedicine Nanotechnology. Biol Med* 8: 767-775.
- MARTINS VL, CALEY M & O'TOOLE EA. 2013. Matrix metalloproteinases and epidermal wound repair. *Cell Tissue Res* 351: 255-268.
- MCKELVEY K, JACKSON CJ & XUE M. 2014. Activated protein C: A regulator of human skin epidermal keratinocyte function. *World J Biol Chem* 5: 169-179.
- NIKPASAND A & PARVIZI MR. 2019. Evaluation of the Effect of Titanium Dioxide Nanoparticles/Gelatin Composite on

Infected Skin Wound Healing; An Animal Model Study. *Bull Emerg Trauma* 7: 366-372.

ORTEGA-GÓMEZ A, PERRETTI M & SOEHNLEIN O. 2013. Resolution of inflammation: An integrated view. *EMBO Mol Med* 5: 661-674.

OSUMI K, MATSUDA S, FUJIMURA N, MATSUBARA K, KITAGO M, ITANO O, OGINO C, SHIMIZU N, OBARA H & KITAGAWA Y. 2017. Acceleration of wound healing by ultrasound activation of TiO<sub>2</sub> in *Escherichia coli*-infected wounds in mice. *J Biomed Mater Res - Part B Appl Biomater* 105: 2344-2351.

OTERO-GONZÁLEZ L, GARCÍA-SAUCEDO C, FIELD JA & SIERRA-ÁLVAREZ R. 2013. Toxicity of TiO<sub>2</sub>, ZrO<sub>2</sub>, Fe<sub>0</sub>, Fe<sub>2</sub>O<sub>3</sub>, and Mn<sub>2</sub>O<sub>3</sub> nanoparticles to the yeast, *Saccharomyces cerevisiae*. *Chemosphere* 93:1201-1206.

PARRA S, OLIVERO J, PACHECO L & PULGARIN C. 2003. Structural properties and photoreactivity relationships of substituted phenols in TiO<sub>2</sub> suspensions. *Appl Catal B Environ* 43: 293-301.

PINTO NCC, CASSINI-VIEIRA P, SOUZA-FAGUNDES EM, DE BARCELOS LS, CASTAÑÓN MCMN & SCIO E. 2016. *Pereskia aculeata* Miller leaves accelerate excisional wound healing in mice. *J Ethnopharmacol* 194: 131-136.

PROCHOWICZ D, KORNOWICZ A & LEWIŃSKI J. 2017. Interactions of Native Cyclodextrins with Metal Ions and Inorganic Nanoparticles: Fertile Landscape for Chemistry and Materials Science. *Chem Rev* 117: 13461-13501.

RASBAND W. 2011. Image J, U. S. National Institutes of Health, Bethesda, Maryland, USA. Available at: <http://rsb.info.nih.gov/ij>.

REIS ÉM, REZENDE AAA, DE OLIVEIRA PF, DE NICOLELLA HD, TAVARES DC, SILVA ACA, DANTAS NO & SPANÓ MA. 2016. Evaluation of titanium dioxide nanocrystal-induced genotoxicity by the cytokinesis-block micronucleus assay and the *Drosophila* wing spot test. *Food Chem Toxicol* 96: 309-319.

REYES-CORONADO D, RODRÍGUEZ-GATTORNO G, ESPINOSA-PESQUEIRA ME, CAB C, DE COSS R & OSKAM G. 2008. Phase-pure TiO<sub>2</sub> nanoparticles: anatase, brookite and rutile. *Nanotechnology* 19: 145605.

SAGHIRI MA, ASATOURIAN A & SHEIBANI N. 2015a. Angiogenesis in regenerative dentistry. *Oral Surg Oral Med Oral Pathol Oral Radiol* 1: 122.

SAGHIRI MA, ASATOURIAN A, SORENSON CM & SHEIBANI N. 2015b. Role of angiogenesis in endodontics: Contributions of stem cells and proangiogenic and antiangiogenic factors to dental pulp regeneration. *J Endod* 41: 797-803.

SANKAR R, DHIVYA R, SHIVASHANGARI KS & RAVIKUMAR V. 2014. Wound healing activity of *Origanum vulgare* engineered titanium dioxide nanoparticles in Wistar Albino rats. *J Mater Sci Mater Med* 25: 1701-1708.

SCHILLING K, BRADFORD B, CASTELLI D, DUFOUR E, NASH JF, PAPE W, SCHULTE S, TOOLEY I, VAN DEN BOSCH J & SCHELLAUF F. 2010. Human safety review of "nano" titanium dioxide and zinc oxide. *Photochem Photobiol Sci* 9: 495-509.

SEISENBAEVA GA, FROMELL K, VINOGRADOV VASILIIY V, TEREKHOV AN, PAKHOMOV AV, NILSSON B, EKDAHL KN, VINOGRADOV, VLADIMIR V & KESSLER VG. 2017. Dispersion of TiO<sub>2</sub> nanoparticles improves burn wound healing and tissue regeneration through specific interaction with blood serum proteins. *Sci Rep* 7: 1-11.

SIVARANJANI V & PHILOMINATHAN P. 2016. Synthesize of Titanium dioxide nanoparticles using *Moringa oleifera* leaves and evaluation of wound healing activity. *Wound Med* 12: 1-5.

WILGUS TA & WULFF BC. 2014. The Importance of Mast Cells in Dermal Scarring. *Adv Wound Care* 3: 356-365.

WILKINSON HN & HARDMAN MJ. 2020. Wound healing: cellular mechanisms and pathological outcomes: Cellular Mechanisms of Wound Repair. *Open Biol* 10: 200223.

XUE M & JACKSON CJ. 2015. Extracellular Matrix Reorganization During Wound Healing and Its Impact on Abnormal Scarring. *Adv Wound Care* 4: 119-136.

YU H ET AL. 2019. Fabrication of Hybrid Materials from Titanium Dioxide and Natural Phenols for Efficient Radical Scavenging against Oxidative Stress. *ACS Biomater Sci Eng* 5: 2778-2785.

#### How to cite

MOURA FBR ET AL. 2022. TiO<sub>2</sub> Nanocrystals and *Annona crassiflora* Polyphenols Used Alone or Mixed Impact Differently on Wound Repair. *An Acad Bras Cienc* 94: e20210230. DOI 10.1590/0001-37652022020210230.

*Manuscript received on February 13, 2021; accepted for publication on June 15, 2021*

**FRANCYELLE B.R. DE MOURA**<sup>1,2</sup>

<https://orcid.org/0000-0003-2127-4310>

**BRUNO ANTONIO FERREIRA**<sup>1</sup>

<https://orcid.org/0000-0001-8773-6704>

**ELUSCA HELENA MUNIZ**<sup>1</sup>

<https://orcid.org/0000-0002-8964-3103>

**RINARA A. SANTOS<sup>1</sup>**

<https://orcid.org/0000-0002-5086-4320>

**JOSÉ AUGUSTO L. GOMIDE<sup>3</sup>**

<https://orcid.org/0000-0002-4117-2664>

**ALLISSON B. JUSTINO<sup>3</sup>**

<https://orcid.org/0000-0003-3616-6611>

**ANIELLE CHRISTINE A. SILVA<sup>4,5</sup>**

<https://orcid.org/0000-0002-5274-156X>

**NOELIO O. DANTAS<sup>4</sup>**

<https://orcid.org/0000-0001-6752-7382>

**DANIELE L. RIBEIRO<sup>1</sup>**

<https://orcid.org/0000-0002-2800-4084>

**FERNANDA A. ARAÚJO<sup>1</sup>**

<https://orcid.org/0000-0002-3212-7079>

**FOUED S. ESPINDOLA<sup>3</sup>**

<https://orcid.org/0000-0002-6937-1411>

**TATIANA CARLA TOMIOSSO<sup>1,2</sup>**

<https://orcid.org/0000-0001-8518-1688>

<sup>1</sup>Universidade Federal de Uberlândia, Instituto de Ciências Biomédicas, Avenida Pará, 1720, Umuarama, 38400-902 Uberlândia, MG, Brazil

<sup>2</sup>Universidade Estadual de Campinas, Instituto de Biologia, Rua Monteiro Lobato, 255, Barão Geraldo, 13083-862 Campinas, SP, Brazil

<sup>3</sup>Universidade Federal de Uberlândia, Instituto de Biotecnologia, Rua Acre, 1004, Umuarama, 38405-319 Uberlândia, MG, Brazil

<sup>4</sup>Universidade Federal de Alagoas, Laboratório de Novos Nanoestruturados e Funcionais, Instituto de Física, Avenida Lourival Melo Mota, s/n, Tabuleiro do Martins, 57072-900 Maceió, AL, Brazil

<sup>5</sup>Universidade Federal de Alagoas, Programa de Pós-Graduação da Rede Nordeste de Biotecnologia, Avenida Lourival Melo Mota, s/n, Tabuleiro do Martins, 57072-970 Maceió, AL, Brazil

Correspondence to: **Tatiana Carla Tomiosso,**

**Foued Salmen Espindola**

*E-mail: tatianatomiosso@gmail.com, fsespindola@ufu.br*

## Author contributions

The animal experiment as well as the morphological and biochemical experiments were conducted by the authors F.B.R.M., B.A.F., E.H.L., R.A.S., J.A.L.A and A.B.J. A.C.A.S. and N.O.D. synthesized and characterized the nanoparticle. D.L.R., F.A.A., F.S.E. and T.C.T coordinated the development of the study. All authors contributed to the writing, discussion and review.

